Macromolecules
ARTICLE

Macromolecules **2009**, *42*, 5155–5166 **5155**
DOI: 10.1021/ma900478n

Using Click Chemistry To Fabricate Ultrathin Thermoresponsive Microcapsules through Direct Covalent Layer-by-Layer Assembly

Cheng-Jyun Huang and Feng-Chih Chang*

Institute of Applied Chemistry, National Chiao Tung University, Hsinchu, Taiwan

Received March 5, 2009; Revised Manuscript Received May 4, 2009

ABSTRACT: We report the syntheses of azido- and acetylene-functionalized poly(*N*-isopropylacrylamide) (PNIPAm) copolymers and their use in the fabrication of ultrathin thermoresponsive microcapsules through direct covalent layer-by-layer (LbL) assembly using click chemistry. The clickable copolymers poly[*N*-isopropylacrylamide-*co*-(trimethylsilyl)propargylacrylamide] and poly(*N*-isoropylacrylamide-*co*-3-azideopropylacrylamide) were prepared through atom transfer radical polymerization (ATRP) at 0 °C using a synthesized dansyl-labeled initiator and the CuBr/Me_6TREN (hexamethylated tris[2-(dimethylamino)ethyl] amine) catalyst complex in 2-propanol. After removing the protective trimethylsilyl groups, these clickable PNIPAm copolymers assemble alternately onto azido-modified silica particles in aqueous media through click reactions catalyzed by copper sulfate and sodium ascorbate. After removing the template, the microcapsules remained stable because of the presence of the covalently bonded triazole units; the microcapsules exhibited thermoresponsive and thermoreversible swelling/deswelling behaviors upon changing the temperature of the medium. Adjusting the number of clickable functionalities resulted in changes to the degree of cross-linking, thereby allowing control over the surface morphology and thickness of the covalently stabilized PNIPAm multilayer thin films. The microcapsules fabricated close to the lower critical solution temperature of PNIPAm exhibited extremely low surface roughnesses and thick multilayer films as a result of their compact chain conformation in aqueous solution, leading to tighter packing of the PNIPAm structure. We further postfunctionalized the surface of the multilayer thin film through click reactions with an azido-modified lissamine rhodamin dye to demonstrate the feasibility of further modification with potentially useful functionalities. Finally, preliminary study on the permeability of microcapsules was presented by using different molecular weigh tetramethylrhodamine isothiocyanate (TRITC)-labeled dextran and rhodamine 6G as probe molecules, and the results revealed that the microcapsules with tighter packing wall are selectively permeable to molecules and show potential applications for the encapsulation of a variety of materials.

Introduction

In recent years, functional hollow spheres—referred to as capsules or vesicles—with well-defined structures and tailorable properties have attracted intense research interest because of the variety of their potential applications, such as in delivery vesicles for drugs,[1] protection shield for proteins, enzymes, and DNA,[2] and catalysis.[3] For many potential applications, microcapsules that are environmentally sensitive to light,[4] temperature,[5] or pH[6] are required to control the transport and delivery of guest materials into their hollow spheres.

For over a decade, the layer-by-layer (LbL) assembly has been a versatile method for the fabrication of hollow capsules.[7] Since its first introduction in the early 1990s,[8] the LbL method has been widely used to deposit multilayers of various materials (e.g., peptides, oligonucleotides, and inorganic nanoparticles) onto colloidal supports.[9] Typically, LbL films are assembled through the alternate deposition of oppositely charged polyelectrolytes (PEs), with the buildup primarily facilitated through electrostatic forces. After the formation of PEs multilayers, the templates are removed to yield hollow capsules. So far, the field of LbL assembly has expanded to include films prepared using other nonelectrostatic interactions—such as hydrogen bonding,[10] host−guest interactions,[11] and hybridization of DNA base pairs[12]—to fabricate hollow capsules.

*Corresponding author. E-mail: changfc@mail.nctu.edu.tw.

The use of covalent bonds to assemble LbL films has several significant advantages over traditional assembly methods because the stability of the resulting cross-linked polymer networks makes them good candidates for special applications. Covalent assembly multilayers of planar substrates has been performed using a variety of reactions between different kinds of functional molecules.[13] These studies have confirmed the benefits of covalent bonding LbL assembly, providing systems that are stable under a range of conditions. For colloidal curved surfaces, postmodifications are often applied—through oxidization,[14] UV irradiation,[15] carbodiimide formation,[16] and glutaraldehyde modification[17]—to enhance the capsules' binding strength in multilayers. There are relatively few reports describing the use of the LbL method to directly deposit covalently bonded multilayer thin films onto the colloidal templates.[18]

Recently, direct covalent assembly on colloidal particles has been performed through the reactions of complementary functional polymers, for example, poly(allylamine hydrochloride) (PAH) and poly(glycidyl methyl acrylate), which react through their amino and epoxide functionalities, respectively.[18a] Single-component polyelectrolyte microcapsules have also been reported from the glutaraldehyde-mediated direct covalent assembly of PAH onto $MnCO_3$ particles.[18b] In addition, a novel method has been introduced to create pH-sensitive degradable capsules based on poly(methacrylic acid) cross-linked via disulfide linkages.[19] These strategies have opened the door to the fabrication of directly covalently bonded multilayer films.

Published on Web 05/29/2009

Recently, a general click chemistry approach[20] for the direct covalent LbL assembly of polymer films onto particles has been developed to create a new class of ultrathin, single-component poly(acrylic acid) (PAA) pH-responsive microcapsules. The development of click chemistry[21] employing the highly efficient copper(I)-catalyzed Huisgen 1,3-dipolar cycloaddition[22] between azides and acetylenes affords superior regioselectivity and almost quantitative transformation under mild conditions with virtually no side reactions or byproducts. Moreover, the resultant aromatic 1,2,3-triazoles linkages are extremely stable making the reaction of particular interest for the formation of covalently linked multilayer thin films. This strategy suggests the potential of using click chemistry techniques for the direct covalent LbL assembly of polymer multilayers on colloidal templates and subsequent formation of single-component capsules.

Poly(*N*-isopropylacrylamide) (PNIPAm) is perhaps the most widely studied thermoresponsive polymer. In aqueous media, PNIPAm exhibits a lower critical solution temperature (LCST) of ca. 32 °C.[23] Below the LCST, the polymer is fully soluble in water because of the formation of hydrogen bonds between water molecules and the polymer's amide side chains. As the temperature is increased, the polymer undergoes a "coil-to-globule" phase transition[24] as a result of the disruption of these hydrogen bonds as well as the release of hydrophobically structured water around the isopropyl groups. One of the earliest processes for making hollow thermosensitive spheres was developed by Zha et al., who used the colloid-templated polymerization of cross-linked PNIPAm shells on silica particles presenting polymerizable units on their surfaces; the subsequent hollow spheres were obtained after dissolving the silica particles in hydrofluoric acid (HF) solution.[25] Since then, many other techniques have been developed to fabricate thermoresponsive hollow spheres based on PNIPAm, including precipitation polymerization,[26] LbL assembly,[27] and interfacial polymerization.[28] Because PNIPAm is uncharged, the use of secondary, nonelectrostatic interactions is vital for its LbL assembly into functional films with nanoscale precision.

In recent years, an extensive range of new polymeric materials for macromolecular engineering and biological applications have been developed using a combination of click chemistry and controlled radical polymerization (CRP).[29] There are many CRP methods for incorporating clickable functionalities into a polymer side chain, including ring-opening metathesis polymerization (ROMP),[30] nitroxide-mediated polymerization (NMP),[31] living cationic ring-opening polymerization,[32] atom transfer radical polymerization (ATRP),[33] and ring-opening polymerization (ROP).[34] Among these techniques, ATRP has several advantages when combined with click chemistry, such as good tolerance toward most functional groups and excellent manipulation of the polymer architecture.

In this paper, we report a method for the fabrication of thermoresponsive microcapsules through direct covalent LbL assembly via click chemistry using clickable azido- and acetylene-functionalized PNIPAm copolymers. Recently, Matyjaszewski et al.[33a] reported that azide moieties are compatible with ATRP, and Hawker et al.[31] demonstrated that pendant acetylene-functionalized copolymer can be prepared through NMP. On the basis of these results, we investigated the copolymerization of poly[*N*-isopropylacrylamide-*co*-(trimethylsilyl)propargylacrylamide] [PNIPAm-*co*-(TMS)Ace] and poly(*N*-isoropylacrylamide-*co*-3-azideopropylacrylamide) (PNIPAm-*co*-Az) using ATRP techniques with a synthesized dansyl-labeled ATRP initiator. After removing the protective trimethylsilyl group, the clickable PNIPAm copolymers were able to assemble alternately onto azido-modified silica particles in aqueous media using click reactions catalyzed by copper sulfate and sodium ascorbate. Using copolymers containing 10 and 20 mol % contents of clickable functionalities (azide and acetylene units), we examined the effect of the degree of cross-linking on the preparation of microcapsules containing multilayer thin films. In addition to this effect, we found that the LbL assembly temperature also significantly influences the morphology and thickness of the multilayer thin films, depending on the conformation of the PNIPAm chains in aqueous solution. The growth of the PNIPAm-Ace/PNIPAm-Az clicked multilayer thin films on silica particles was monitored by measuring their fluorescence intensities using confocal laser scanning microscopy (CLSM). Furthermore, we also characterized the microcapsules using transmission electron microscopy (TEM) and atomic force microscopy (AFM) in the tapping mode. Taking advantage of the LCST characteristics of PNIPAm, we also used AFM and TEM to examine the thermoresponsive behavior of the swelling and deswelling of the microcapsules upon elevating the temperature of the medium. Finally, we demonstrate the feasibility of postfunctionalization of the microcapsules through the reaction of an azido-modified lissamine rhodamine dye with the remaining excess of free acetylene functional groups of the surface of the multilayer thin films.

Experimental Section

Materials. The following reagents and solvents were purchased from commercial suppliers and used as received unless otherwise noted: L-ascorbic acid sodium salt (TCI, >98%), bromoisobutyryl bromide (ACROS, 98%), acryloyl chloride (Alfa Aesar, 96%), 3-bromopropyltrichlorosilane (Aldrich, 96%), cupric sulfate pentahydrate (SHOWA, 99.5%), chlorotrimethylsilane (Lancaster, 98+%), 3-chloropropylamine hydrochloride (ACROS, 98%), dansyl chloride (ACROS, 98%), *N*,*N*-diisopropylethylamine (DIPEA) (ACROS, 98%), 1,8-diazabicyclo[5.4.0]undec-7-ene (DBU; ACROS, 98%), propargylamine (ACROS, 99%), rhodamine 6G (Aldrich, ~95%), tetrabutylammonium fluoride (1 M solution in THF; ACROS), tetramethylrhodamine isothiocyanate (TRITC)-labeled dextran (M_w ~ 4400, 65 000−76 000 g mol^{-1}) (Aldrich), silver chloride (ACROS, 99+%), sodium azide (SHOWA, 98%), and 2-propanol (Tedia, 99.5%). The monomer *N*-isopropylacrylamide (NIPAm, 99%, TCI) was recrystallized from hexane/toluene and dried under vacuum prior to use. *N*,*N*-Dimethylformamide (DMF) (Tedia, 99.8%) and toluene (Tedia, 99.5%) were dried over CaH_2 (ACROS, 93%) and distilled under reduced pressure. Tetrahydrofuran (Tedia, 99.8%) was distilled over Na/benzophenone. The deionized (DI) water used in all reactions, solution preparations, and polymer isolations was purified to a resistance of 18 MΩ (Milli-Q Reagent Water System, Millipore Corp.). Silica particles (diameter: 3 μm) were obtained from Polysciences, Inc. Hexamethylated tris[2-(dimethylamino)ethyl]amine (Me_6TREN) was synthesized according to the method described by Ciampolini.[35] Copper(I) bromide (Acros, 98%) was washed with glacial acetic acid to remove any soluble oxidized species, and then it was filtered, washed with ethanol, and dried. (Trimethylsilyl)propargylacrylamide,[31] 1-azido-3-aminopropane,[36] azido-modified lissamine rhodamine (LRAz),[37] and $Cu(PPh_3)_3Br$[38] were synthesized using previously described procedures.

Characterizations. Analytical TLC was performed on commercial Merck Plates coated with silica gel GF254 (0.24 mm thick). Silica gel for flash chromatography was Merck Kieselgel 60 (230−400 mesh, ASTM). ^{1}H NMR (500 MHz) and ^{13}C NMR (125 MHz) were recorded using a Varian Unity Inova spectrometer using $CDCl_3$ or D_2O as the solvent. Fourier transform infrared (FT-IR) spectra of solid samples were recorded at room temperature using a Nicolet AVATAR 320 FT-IR spectrometer. Gel permeation chromatography (GPC) was performed a Hitachi L-7100 pump and a RI 2000 refractive index detector (Schambeck SFD GmbH); the elution rate was 1.0 mL/min and the temperature was 80 °C; a Polymer Laboratories PLgel guard column (5 μm particles; 50 × 7.5 mm) and a PLgel 5 μm

Mixed-D column (300 × 7.5 mm; particle size: 5 μm) were connected in series. The molecular weight calibration curve was obtained using poly(ethylene oxide) standards of defined molecular weights (1010−163 000 g/mol) (Polymer Laboratories Inc., Amherst, MA). TEM images were obtained using a JEOL TEM-1200EX II instrument operated at 120 kV. Height measurements of the microcapsules were determined using tapping-mode AFM (Digital Instrument NS4/D3100CL/MultiMode AFM; Veeco-Digital Instruments, Santa Barbara, CA) with silicon cantilevers (Pointprobe Silicon AFM Probe) at room temperature, in air. The swelling samples of PNIPAm microcapsules were prepared by drying a droplet of capsule suspension on the surface of a clean silicon wafer or copper grid and allowing it to dry freely in air. In order to maintain its shrunk morphology, the deswelling samples were prepared by heating the capsules suspension solution up to 50 °C for 20 min and allowing a droplet of heated capsule suspension to be dried quickly in this oven at 50 °C on silicon wafer or copper grid. CLSM and DIC (differential interference contrast) images were recorded using a Leica TCS SP5 confocal microscope imaging system equipped with a diode laser (excitation wavelength: 403 and 561 nm) to quantify the fluorescence of the coated particles. Thermal analyses of the homo- and copolymer solutions were performed using a Q-20 calorimeter (TA Instruments, New Castle, DE). Heating scans were recorded in the range of 0−50 °C at a scan rate of 2 °C min^{-1}.

Propargyl 2-Bromo-2-methylpropionamide (1). A solution of propargylamine (6.00 g, 5.45 mmol) and triethylamine (11.4 mL, 8.18 mmol) dissolved in THF (300 mL) was fed into a 500 mL two-necked round-bottom flask equipped with an Ar inlet and a rubber septum and then cooled in an ice bath. After adding α-bromoisobutyryl bromide (12.5 g, 5.45 mmol) dropwise to the solution, a white precipitate of triethylammonium bromide was formed. The mixture was stirred at room temperature overnight, the precipitate was filtered off, the solvent was evaporated, and the crude product was purified through column chromatography (*n*-hexane/EtOAc, 4:1) to give **1** as a pale yellow solid (7.84 g, 70.5%). ^{1}H NMR (500 MHz, $CDCl_3$), δ_H: 6.88 (br s, 1H, N**H**), 4.05 (dd, J = 5.25, 2.57 Hz, 2H, CC**H**$_2$NH), 2.27 (t, J = 2.56 Hz, 1H, C**H**≡C), 3.37 [s, 6H, C(C**H**$_3$)$_2$Br]. ^{13}C NMR (125 MHz, $CDCl_3$), δ_C: 171.7 (**C**O), 78.8 (CH≡**C**), 72.0 (**C**H≡C), 62.2 [**C**C(CH$_3$)$_2$Br], 32.4 [(**C**H$_3$)$_2$Br], 30.3 (C**C**H$_2$NH).

5-(Dimethylamino)naphthalene-1-sulfonic Acid (3-Azidopropyl)amide (Dansyl-N$_3$, 2). 1-Azido-3-aminopropane (2.23 g, 2.67 mmol) was added to a solution of dansyl chloride (4.00 g, 14.8 mmol) in dry THF (100 mL). Triethylamine (3 mL) was added, and then the mixture was stirred at room temperature for 16 h. The solvent was evaporated under vacuum, and the crude product was purified through column chromatography (EtOAc) to give **2** as a yellow oil (3.78 g, 76.5%). ^{1}H NMR (500 MHz, $CDCl_3$) δ_H: 8.56 (d, J = 8.49 Hz, 1H, Ar**H**), 8.28−8.24 (m, 2H, Ar**H**), 7.58 (t, J = 8.10 Hz, 1H, Ar**H**), 7.54 (t, J = 7.50 Hz, 1H, Ar**H**), 7.20 (d, J = 7.53 Hz, 1H, Ar**H**), 4.90 (br s, 1H, N**H**), 3.26 (t, J = 6.40, 2H, CH$_2$C**H**$_2$N$_3$), 2.98 (q, J = 6.44 Hz, 2H, NHC**H**$_2$CH$_2$), 2.90 [s, 6H, N(C**H**$_3$)$_2$], 1.67−1.60 (m, 2H, CH$_2$C**H**$_2$CH$_2$). ^{13}C NMR (125 MHz, $CDCl_3$), δ_C: 152.1, 134.3, 130.6, 129.9, 129.8, 129.5, 128.5, 123.2, 118.5, 115.3 (naphthalene carbons), 48.8 (**C**H$_2$N$_3$), 45.4 [N(**C**H$_3$)$_2$], 40.8 (NH**C**H$_2$), 28.8 (CH$_2$**C**H$_2$CH$_2$).

Dansyl-Labeled ATRP Initiator (3). *N*,*N*-Diisopropylethylamine (0.075 g, 5.2 mmol) and Cu(PPh$_3$)$_3$Br (223 mg, 2.40 μmol) were added to a solution of propargyl 2-bromo-2-methylpropionamide (**1**; 2.45 g, 1.20 mmol) and dansyl-N$_3$ (**2**; 4.00 g, 1.20 mmol) in THF (30 mL), and then the mixture was stirred at room temperature for 12 h. The solvent was evaporated, and the crude product was purified through column chromatography (*n*-hexane/EtOAc, 2:1) to give **3** as a yellow solid (5.76 g, 89.5%). ^{1}H NMR (500 MHz, $CDCl_3$), δ_H: 8.56 (d, J = 8.41 Hz, 1H, Ar**H**), 8.28 (d, J = 8.59 Hz, 1H, Ar**H**), 8.18 (d, J = 9.29 Hz, 1H, Ar**H**), 7.51 (m, 2H, Ar**H**), 7.47 (s, 1H, triazole *H*), 7.20 (d, J = 7.55 Hz, 1H, Ar**H**), 5.78 (br s, 1H, N**H**), 4.47 (d, J = 5.04 Hz, CC**H**$_2$NH, 2H), 4.33 (t, J = 6.11 Hz, 2H, CH$_2$C**H**$_2$N), 2.89 [s, 6H, N(CH$_3$)$_2$], 2.87 (m, 2H, NHC**H**$_2$CH$_2$), 2.92−2.81 (m, 2H, CH$_2$C**H**$_2$CH$_2$), 1.90 [s, 6H, C(C**H**$_3$)$_2$Br]. ^{13}C NMR (125 MHz, $CDCl_3$), δ_C: 172.2 (**C**ONH), 151.4 (**C**N(CH$_3$)$_2$), 144.1 (**C**CH$_2$NH), 134.5, 130.5, 129.7, 129.6, 129.5, 128.5, 123.4, 122.9 119.0 (naphthalene carbons), 115.5 (N**C**HC), 62.2 [**C**C(CH$_3$)$_2$Br], 47.1 (**C**H$_2$N), 45.5 [N(**C**H$_3$)$_2$], 39.9 (NH**C**H$_2$CH$_2$), 35.8 (C**C**H$_2$NH), 32.2 [(**C**H$_3$)$_2$Br], 30.1 (CH$_2$**C**H$_2$CH$_2$).

3-Azidopropylacrylamide (4). 1-Azido-3-aminopropane (5.00 g, 5.00 mmol) and triethylamine (10.45 mL, 7.50 mmol) were dissolved in dry CH_2Cl_2 (200 mL) and cooled to 0 °C. Acryloyl chloride (4.53 g, 5.00 mmol) was added slowly over 30 min, and then stirring was continued for an additional 16 h at room temperature. The reaction mixture was washed with brine and water, dried ($MgSO_4$), and concentrated under reduced pressure. The crude product was further purified through column chromatography (*n*-hexane/EtOAc, 1:1) to give **4** as a colorless oil (5.33 g, 69.2%). ^{1}H NMR (500 MHz, $CDCl_3$), δ_H: 6.24 (dd, J = 1, 17 Hz, 1H, trans C**H**$_2$=CH), 6.19 (br s, 1H, N**H**), 6.09 (dd, J = 10.5, 17 Hz, 1H, CH$_2$=C**H**), 5.61 (dd, J = 1, 10.5 Hz, 1H, cis C**H**$_2$=CH), 3.40−3.38 (br m, 4H, C**H**$_2$CH$_2$C**H**$_2$−N$_3$), 1.82−1.77 (m, 1H, C**H**$_2$CH$_2$−N$_3$). ^{13}C NMR (125 MHz, $CDCl_3$), δ_C: 165.8 (**C**=O), 130.7 (CH$_2$=**C**H), 126.5 (**C**H$_2$=CH), 49.3 (CH$_2$**C**H$_2$−N$_3$), 37.1 (NH−**C**H$_2$), 28.7 (CH$_2$**C**H$_2$CH$_2$).

Trimethylsilyl-Protected Acetylenic Acrylamide Copolymers {Poly[NIPAm-*co*-(trimethylsilyl)propargylacrylamide], 5}. NIPAm (2.32 g, 2.05 mmol), (trimethylsilyl)propargylacrylamide (0.93 g, 0.51 mmol), and the dansyl-labeled initiator (0.069 g, 1.28 μmol) were mixed at a 180:20:1 molar ratio in 2-propanol (2.5 mL). The solution was deoxygenated by performing freeze/pump/thaw cycles. Upon equilibration at 20 °C after the third cycle, the flask was immersed in an ice bath. An oxygen-free solution of 2-propanol (1.00 mL) containing CuBr (0.0184 g, 1.28 μmol) and Me$_6$TREN (29.65 mg, 35.00 μL) was prepared separately. This solution was added to the monomer/initiator mixture through an argon-purged syringe to initiate the polymerization; stirring was performed for an additional 12 h. The reaction mixture was exposed to air to terminate the polymerization; the sample was then evaporated to dryness, and the residue dissolved in THF (50 mL). The copper catalyst was removed by passing the solution through a neutral alumina column. The eluate was concentrated and added to *n*-hexane to precipitate **5**, which was collected as a pale yellow powder. ^{1}H NMR (500 MHz, $CDCl_3$), δ_H: 0.13 [br s, Si(C**H**$_3$)$_3$], 1.12 [br s, CH(C**H**$_3$)$_2$], 1.38−2.14 (br m, polymer backbone), 3.98 [br s, C**H**(CH$_3$)$_2$].

Acetylenic Acrylamide Copolymers {Poly(NIPAm-*co*-propargylacrylamide, 6}. Excess tetrabutylammonium fluoride was added to a solution of poly[NIPAm-*co*-(trimethylsilyl)propargylacrylamide] in dry THF to 0 °C. The mixture was then stirred for 2 h at 0 °C. The solution was dialyzed extensively against DI water, and the product was isolated via lyophilization to give **6** as a pale yellow powder. ^{1}H NMR (500 MHz, D_2O), δ_H: 1.08 [br s, CH(C**H**$_3$)$_2$], 1.25−1.77 (br m, C**H**$_2$CH, copolymer backbone), 1.78−2.22 (br m, CH$_2$C**H** polymer backbone and C≡C**H**) 3.71−3.97 [br m, C**H**(CH$_3$)$_2$ and NHC**H**$_2$C].

Azido-Functionalized PNIPAm Copolymers {Poly(NIPAm-*co*-3-azidopropylacrylamide, 7}. NIPAm (1.95 g, 1.73 mmol), 3-azidopropylacrylamide (0.67 g, 0.43 mmol), and the dansyl sulfonyl azide amide ATRP initiator (0.058 g, 1.08 μmol) were dissolved at an approximate 180:20:1 molar ratio in 2-propanol (1.5 mL), and then the solution was deoxygenated by performing freeze/pump/thaw cycles. Upon equilibration at 20 °C after the third cycle, the flask was immersed in an ice bath. An oxygen-free solution of 2-propanol (0.5 mL) containing CuBr (0.0155 g, 1.08 μmol) and Me$_6$TREN (24.99 mg, 29.68 μL) was prepared separately. This solution was added to the monomer/initiator mixture through an argon-purged syringe to initiate the polymerization; the mixture was then stirred for 12 h.

Scheme 1. Synthesis of the Fluorescent Amide-Linked Dansyl-Labeled ATRP Initiator 3 Using a Click Reaction; Preparation of Acetylene- and Azido-Functionalized PNIPAm Random Copolymers Using ATRP

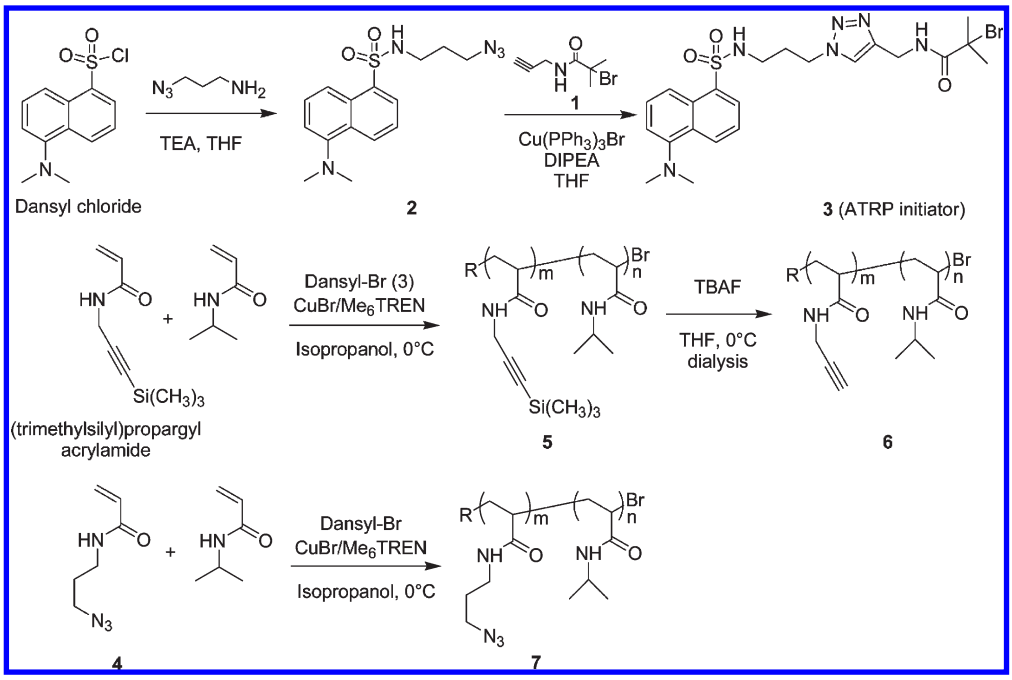

The reaction mixture was exposed to air to stop the polymerization; after evaporation to dryness, the residue was dissolved in THF (30 mL), and the copper catalyst was removed by passing the solution through a neutral alumina column. The eluate was concentrated and added to *n*-hexane to precipitate **7**, which was collected as a pale yellow powder (1.95 g, 42.3%). ^{1}H NMR (500 MHz, D_2O), δ_H: 1.08 [br s, $CH(CH_3)_2$], 1.26−1.78 (m, CH_2CH polymer backbone and $NHCH_2CH_2$), 1.79−2.16 (br m, CH_2CH polymer backbone), 2.82 (br s, $N(CH_3)_2$ from initiator), 3.08−3.26 (br m, $NHCH_2$), 3.27−3.36 (br m,CH_2N_3), 3.83 [br s, $CH(CH_3)_2$].

3 μm Azido-Modified Silica Particles. [39] Anhydrous toluene (7 mL) was added under an Ar atmosphere to a Schlenk flask containing 3 μm silica microparticles (500 mg), and then the flask was placed into an oil bath at 80 °C. After stirring for 30 min, a solution of 3-bromopropyltrichlorosilane (0.5 mL) in anhydrous toluene (3 mL) was added dropwise, and then the mixture was maintained at 80 °C for an additional 18 h. After centrifuging and removal of the supernatant solution, the particles were washed three times with toluene and ethanol to remove excess bromopropyltrichlorosilane, and then the product bromo-modified silica particles were dried under reduced pressure. A sample of the bromo-modified silica particles (300 mg) was combined with sodium azide (1.0 g) in DMF (5 mL), and then the suspension was stirred at 80 °C for 18 h. After centrifugation and removal of the supernatant, the product was washed three times with distilled water, acetone, and ethanol and then dried under reduced pressure.

General Procedure for Direct Covalent LbL Assembly of PNIPAm Multilayer Thin Films on Azido-Modified Silica Particles. An aqueous solution (4 mL) containing the azide-modified silica particles (10 mg) and the acetylene-functionalized PNIPAm copolymers (5 mg) was combined with copper(II) sulfate (2 mg). The suspension was sonicated for 5 min, sodium ascorbate solution (5 mg/mL, 1 mL) was added, and then the mixture was incubated for 8 h at 25 °C. After the click reaction was complete, the dispersion of particles was centrifuged and the supernatant was removed and replaced with DI water. This rinsing process, aided by ultrasonication, was repeated three times to ensure removal of the excess copolymer; at this point, the next copolymer solution was added to the dispersion. Upon the addition of the sodium ascorbate solution, the reaction mixture turned brownish for the azide-functionalized PNIPAm copolymer solution and yellowish for the acetylene-functionalized PNIPAm copolymer solution; this color persisted for several hours. To ensure that the clickable groups on the thin film's surface were completely consumed and covered by the deposited copolymers, the mixtures were stirred for at least 8 h until the solution had turned pale blue, signifying the reaction's completion. After the desired number of bilayers had been formed, the microcapsules were obtained by immersing the coated silica particles in 2 M HF for 5 min at ambient temperature to etch out the silica cores completely. The resulting microcapsules were purified through extensive dialysis against DI water.

Postfunctionalization of Multilayer Thin Films. The three-layer (PNIPAm-Ace_{22}/PNIPAm-Az_{10})PNIPAm-Ace_{22}-coated silica particles (1.25 mg/mL, 4 mL) were combined with copper(II) sulfate pentahydrate (2 mg) and LRAz dye (5 mg). Sodium ascorbate (5 mg) in DI water (1.0 mL) was then added to the mixture, which was then incubated for 6 h. The particles were dialyzed extensively with DI water until no fluorescence was detectable in the supernatant.

Results and Discussion

ATRP Synthesis and Characterization of Clickable Thermoresponsive PNIPAm Copolymers. To incorporate clickable functionalities and take advantage of click chemistry for the direct covalent LbL assembly of multilayer thin films on colloidal particles, our general strategy began with the preparation of thermoresponsive copolymers presenting reactive side-chain substituents from PNIPAm backbones. Bergbreiter and Chance reported water-soluble PNIPAm copolymers featuring pendent azide and acetylene groups for covalent LbL grafting on polyethylene via click reactions; they used conventional free radical copolymerization of NIPAm and acrylate-based comonomers, followed by postfunctionalization, to afford these clickable functionalities.[40] We recently demonstrated the ATRP polymerization of well-defined PNIPAm polymers using an amide-linked initiator.[41] Following similar experimental conditions in this study, we employed two acrylamide-based monomers—3-azidopropylacrylamide[42] (AzPAM) and

Table 1. Characterization Data for the Acetylene- and Azido-Functionalized Copolymers

entry	click-functionalized copolymer sample	$M_{n,GPC}$ (kg/mol)	$M_{n,NMR}$ (kg/mol)	M_w/M_n	F_{azide} [a]	$F_{acetylene}$ [b]	maximum of endothermic peak (°C)
1	PNIPAm$_{138}$-*co*-Ace$_{15}$	13 900	17 200	1.23		9.8	31.5
2	PNIPAm$_{113}$-*co*-Az$_{13}$	13 300	14 800	1.21	10		30.0
3	PNIPAm$_{137}$-*co*-Ace$_{39}$	19 600	19 700	1.25		22	30.9
4	PNIPAm$_{73}$-*co*-Az$_{20}$	9 500	11 300	1.16	22		24.9

[a] F_{azide}: mole percentage of azide functionality. [b] $F_{acetylene}$: mole fraction of acetylene functionality in D_2O at 20 °C, measured using ^1H NMR spectroscopy.

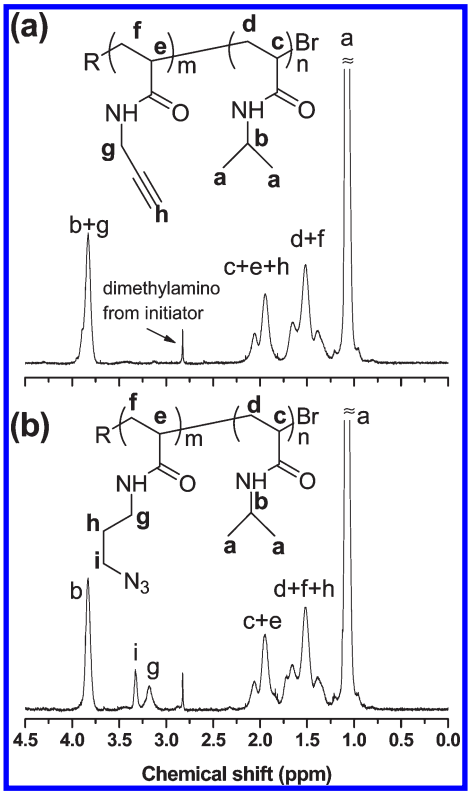

Figure 1. ^1H NMR spectra of (a) PNIPAm-Ace$_{9.8}$ and (b) PNIPAm-Az$_{10}$ in D_2O at 20 °C.

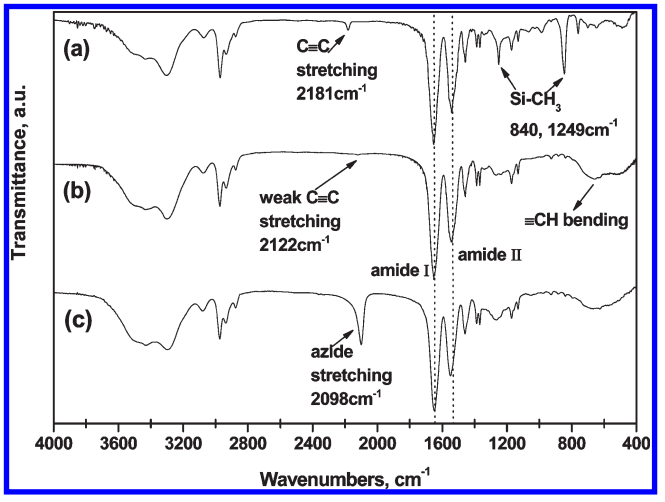

Figure 2. IR spectra of (a) PNIPAm-(TMS)Ace, (b) PNIPAm-Ace, and (c) PNIPAm-Az.

(trimethylsilyl)propargylacrylamide[31]—for ATRP copolymerization with NIPAm, catalyzed by CuBr/Me$_6$TREN, using a synthesized fluorescent amide-linked initiator in isopropyl alcohol at 0 °C (Scheme 1). To incorporate the clickable functionalities into PNIPAm while retaining its

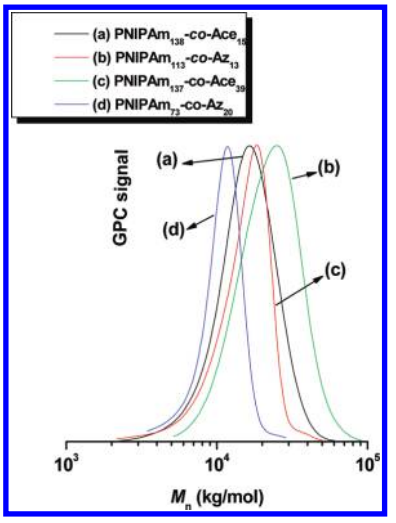

Figure 3. GPC traces of click-functionalized PNIPAm copolymer samples.

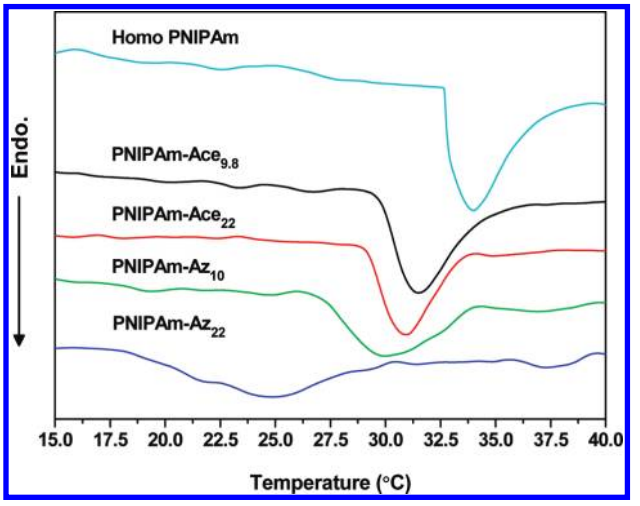

Figure 4. DSC thermorgrams of click-functionalized PNIPAm copolymers and a PNIPAm homopolymer in aqueous solution (1 wt %; heating rate: 2 °C/min).

thermoresponsive behavior, these copolymer materials were designed to contain only 10 and 20 mol % of either the azide or the acetylene functional monomers. Table 1 provides a detailed summary of the results and the polymer characterization. The acetylene unit in the monomer was protected with a trimethylsilyl (TMS) group to circumvent its complexation with the copper catalyst during ATRP copolymerization.[43] After removing this protective group with tetrabutylammonium fluoride (TBAF) in THF, we obtained the desired acetylene-functionalized PNIPAm copolymer. We used ^1H NMR spectroscopy (Figure 1) to determine the number of repeating units (from the relative integration of the peaks of the dimethylamino protons of the initiator) and the composition of copolymers (by comparing the

Scheme 2. Schematic Representation of the Preparation of Covalently Stabilized Thermoresponsive Microcapsules Through Layer-by-Layer Assembly Using Click Chemistry

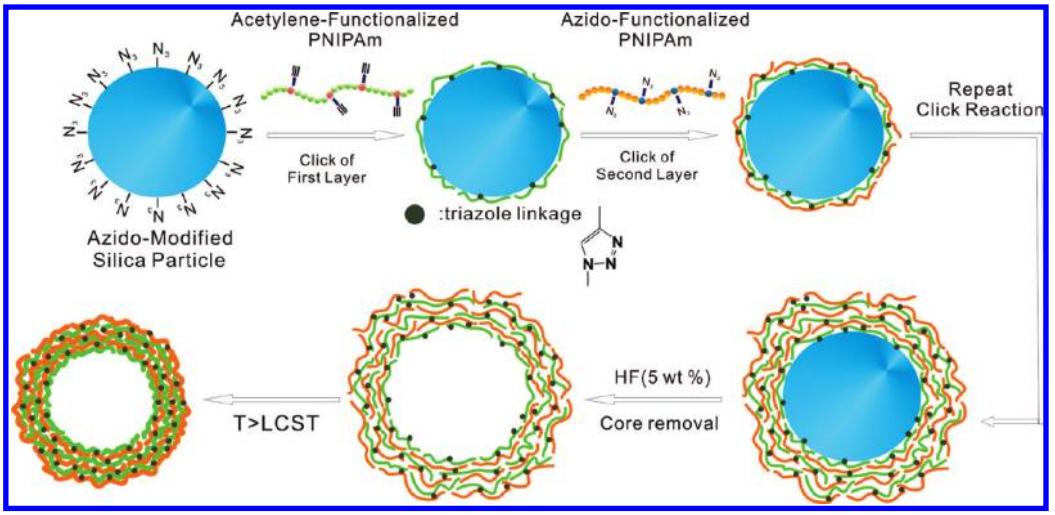

integration of the signals of the methylene protons neighboring to the azido groups and with methyl protons of TMS). We found that the compositions of the azide and acetylene moieties were very close to their monomer contents of 10 and 20 mol %; we denote these samples as PNIPAm-Ace$_a$ and PNIPAm-Az$_a$, where a represents the molar percentage of clickable functionalities in the copolymers. Figure 2 displays the FT-IR spectra of the copolymers, revealing the characteristic absorptions of the TMS-protected acetylene, the fingerprint weak acetylene, and the strong azide peaks at ca. 2181, 2122, and 2098 cm^{-1}, respectively. The GPC traces in Figure 3 display clear monomodal and symmetric peaks, without any discernible tailing or shoulders at the lower or higher molecular weight side. These data reveal that we had successfully prepared the click-functionalized PNIPAm copolymers through ATRP.

The LCST of PNIPAm copolymers is strongly influenced by the nature and molar concentration of the comonomer and by the overall hydrophilicity of the copolymer.[44] In general, hydrophobic compounds lower the LCST, whereas hydrophilic compounds raise it.[45] Figure 4 presents DSC thermograms of our four azido- and acetylene-functionalized samples in relation to that of the homo-PNIPAm. We consider the temperature at the maximum of the DSC endotherm to be the LCST of the copolymer. The transition temperatures of the acetylene-functionalized copolymers were slightly lower than that of the homo-PNIPAm. When the comonomer AzPAM content was 8.7 mol %, however, the transition temperature became broader and the LCST decreased to 30.0 °C, i.e., lower than that of PNIPAm-Ace$_{0.17}$. Furthermore, we observed a much lower and broader LCST region for PNIPAm-Az$_{0.22}$; its LCST was ca. 24.9 °C. This result indicates that by the hydrophobic azide groups and alkyl chains dominate the hydrophilicity over the hydrophilic amide groups in the AzPAM, leading to a decrease in the LCST.[46] In contrast, the shorter propargyl group results in a less hydrophobic copolymer, which, thus, provided less of a change in the LCST. Because aqueous PNIPAm solutions undergo coil-to-globule phase transitions when the temperature is increased, we expected the LbL assembly behavior to depend strongly on the reaction temperature and, hence, the conformation of the copolymer chain.

Click Reactions for the Direct Covalent LbL Assembly of Multilayer Thin Films on Silica Particles. We chose silica particles as our sacrificial template material because of its ready availability over a broad range of sizes with monodispersity and because their surface can be readily modified with silylating agents. We treated the hydroxyl groups on the surface of the particles with an excess of 3-bromopropyltrichlorosilane and then exchanged the bromine atoms into azide groups through nucleophilic substitution with NaN_3 in DMF. Next, we began the LbL assembly at 25 °C, mediated through 1,3-dipolar cycloaddition between the azide units on the surfaces of silica particles and the acetylene-functionalized PNIPAm copolymer, to form the first thin film layer (Scheme 2). Because of the coil-to-globule phase transition, these copolymers adopted coil structures in aqueous solution at temperatures below their LCSTs. We expected that these conformations led to steric restriction, with only a portion of these clickable functionalities of the copolymers being consumed.[20] Consequently, we exploited the remaining free acetylene groups on the surface of the first thin film layer in the next assembly step. Repeating this process provided the desired number of layers on the surface of the silica particles, leaving behind single-component covalently stabilized PNIPAm microcapsules after core removal through HF etching.

We used CLSM to confirm the growth of multilayer thin films on the silica particles by measuring the fluorescence intensities after depositing each bilayer. Figure 5a reveals a steady increase in the fluorescence intensity upon increasing the number of deposited PNIPAm-Ace$_{9.8}$/PNIPAm-Az$_{10}$ layers. The CLSM image in Figure 5b reveals the uniform coverage and regular spherical shape of the dansyl-labeled copolymers on the silica particle templates, confirming the buildup of multilayer thin films on the particles. The AFM images in Figure 5c display the continuous morphology and intact shell structure of the microcapsules after removal of the template. We observe creases and folds, which are characteristic of ultrathin walls resulting from collapse of the microcapsules after drying. The TEM images in Figure 5d confirm that these shells retained their integrity after dissolution of the core. We calculated the thickness of the multilayer thin films by examining the AFM height profiles of the microcapsules from regions in which they had folded only once. The thickness of the five-bilayer PNIPAm-Ace$_{9.8}$/PNIPAm-Az$_{10}$ thin film was ca. 5.5 nm. Cross-linking of PNIPAm provides temperature-sensitive polymer networks that swell in water at temperatures below their LCST and

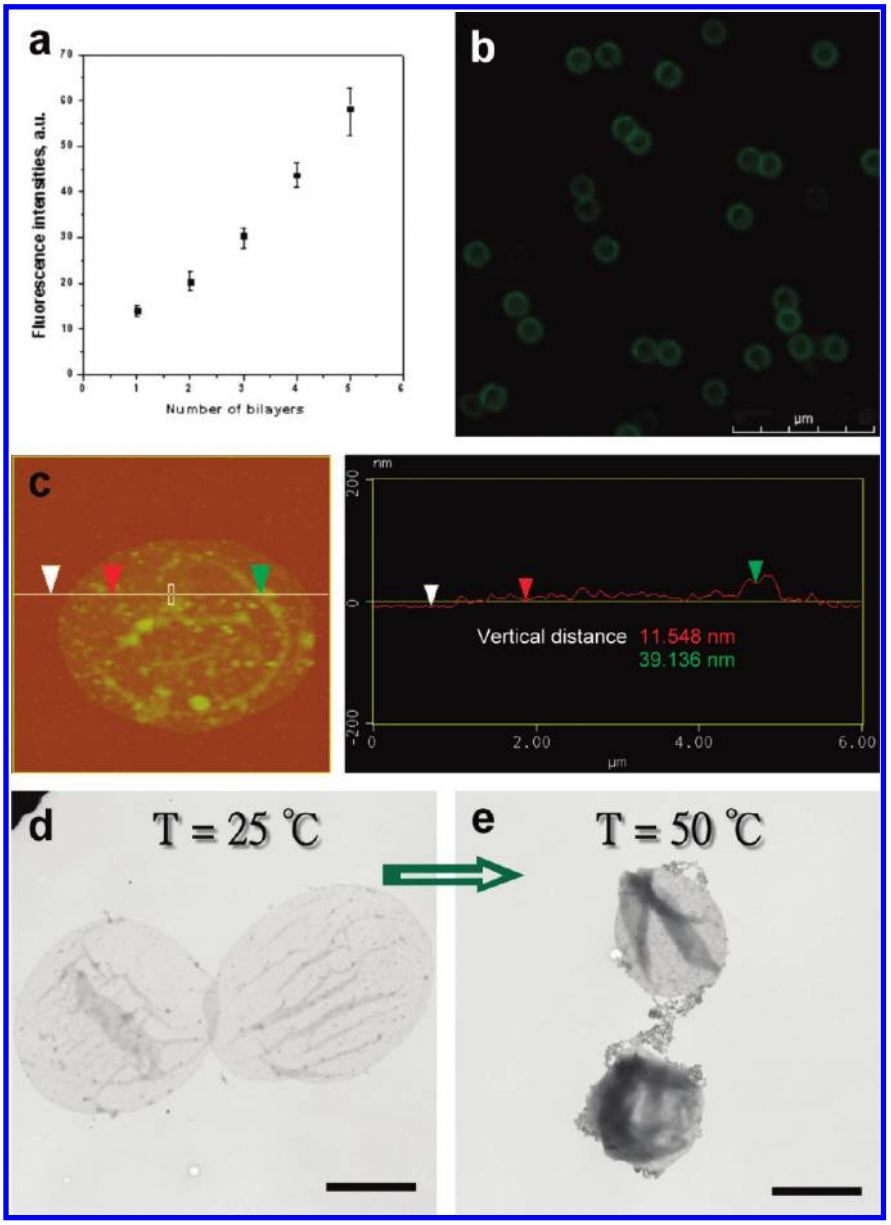

Figure 5. (a) Fluorescence intensity of 3 μm SiO_2 particles plotted as a function of the number of deposited PNIPAm-$Ace_{9.8}$/PNIPAm-Az_{10} bilayers. (b) CLSM image of 3 μm SiO_2 particles featuring five bilayers of PNIPAm-$Ace_{9.8}$/PNIPAm-Az_{10} bilayers in aqueous solution; the scale bar: 20 μm. (c) Tapping-mode AFM image of a collapsed PNIPAm microcapsule (dried state) featuring five PNIPAm-$Ace_{9.8}$/PNIPAm-Az_{10} bilayers; the AFM-derived thickness of the multilayer was measured in terms of the difference in heights at the points marked by the arrows. (d, e) TEM images of (PNIPAm-$Ace_{9.8}$/PNIPAm-Az_{10})$_5$ microcapsules prepared in the (d) dried state and (e) thermally dried state (50 °C); the scale bar: 2 μm.

deswell at temperatures above it.[47] As expected, the sizes of our microcapsules changed dramatically upon increasing the aqueous solution temperature from 25 to 50 °C (Figure 5e). We conducted the LbL assembly in aqueous solutions to observe its thermoresponsive behavior, and the result indicates the success of our click reaction-mediated fabrication of covalently stabilized microcapsules. This novel clickable functionalized PNIPAm derivatives provided the microcapsules with covalent linkages and also retained its thermoresponsive characteristics, thereby allowing them to exhibit swelling and deswelling behavior.

Effect of Cross-Linking Degree on Multilayer Thin Films Thickness and Morphology. To further investigate the properties of the PNIPAm-$Ace_{9.8}$/PNIPAm-Az_{10} multilayer thin films, we fabricated them from copolymers containing various contents of their click functionalities. The AFM images in Figure 6 reveal an increase in the thickness of the films upon increasing the number of bilayers. Because of the instability of the microcapsules containing less than one bilayer, it was difficult to measure the thickness of these systems. The average thickness of the microcapsules assembled from PNIPAm-Ace_{22}/PNIPAm-Az_{10} (Figure 6, circles) was greater than that of its counterparts prepared from PNIPAm-$Ace_{9.8}$/PNIPAm-Az_{10}. For example, two-bilayer microcapsules assembled from PNIPAm-Ace_{22}/PNIPAm-Az_{10} had a thickness of ca. 8 nm, whereas the five-bilayer PNIPAm-$Ace_{9.8}$/PNIPAm-Az_{10} microcapsule was 5.5 nm thick (Figure 5c). This result clearly indicates that the increase in film thickness was influenced by the degree of cross-linking. We found, however, that the increase in thickness was nonlinear—the thickness of the bilayers decreased progressively as the number of deposited bilayers increased. This behavior can be explained by considering that as the multilayer thin films assembled in the second layer, the number of clickable functionalities of the PNIPAm-Az_{10} polymer decreased, leaving an insufficient number of free

clickable azide groups on the surface. As a result, the subsequent LbL assembly was restricted, leading to sequentially thinner bilayers in the multilayer thin films.

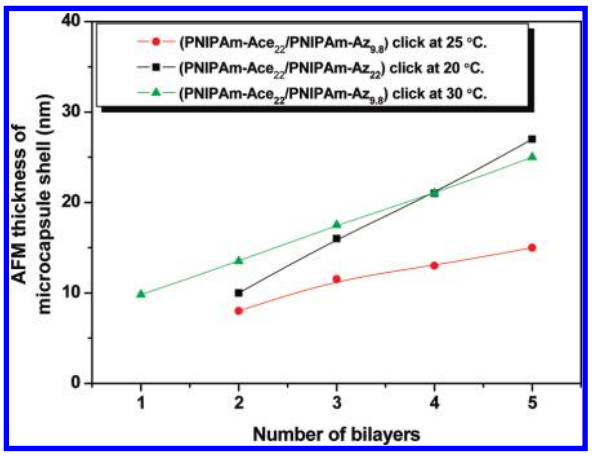

Figure 6. PNIPAm microcapsules multilayer thicknesses—measured using tapping-mode AFM—plotted with respect to the number of bilayers, the cross-linking degree, and the reaction temperature.

As mentioned above, increasing the content of azide functionalities to 22 mol % dramatically lowered the LCST; the copolymer became insoluble in aqueous solution at 25 °C. To avoid serious aggregation, we conducted the buildup of (PNIPAm-Ace_{22}/PNIPAm-Az_{22}) multilayers at 20 °C to examine the effect of higher degrees of cross-linking. We observed a regular increase in the multilayer thickness, providing films that were thicker than those of the (PNIPAm-$Ace_{9.8}$/PNIPAm-Az_{10})$_n$ systems (Figure 6, squares). Thus, the direct covalent LbL multilayer growth also depends on the degree of cross-linking. In addition, we found that the thickness of the microcapsule shells obtained from height measurements increased gradually with respect to the number of bilayers. This behavior confirms unambiguously the success of our direct covalently bonded LbL assembly procedure for the fabrication of microcapsules possessing ultrathin walls. Indeed, the thickness of the microcapsules can be adjusted through control of the degree of cross-linking.

Tailoring Multilayer Thin Film Morphologies by Adjusting the Reaction Temperature. In addition to the degree of cross-linking, the temperature at which LbL assembly of

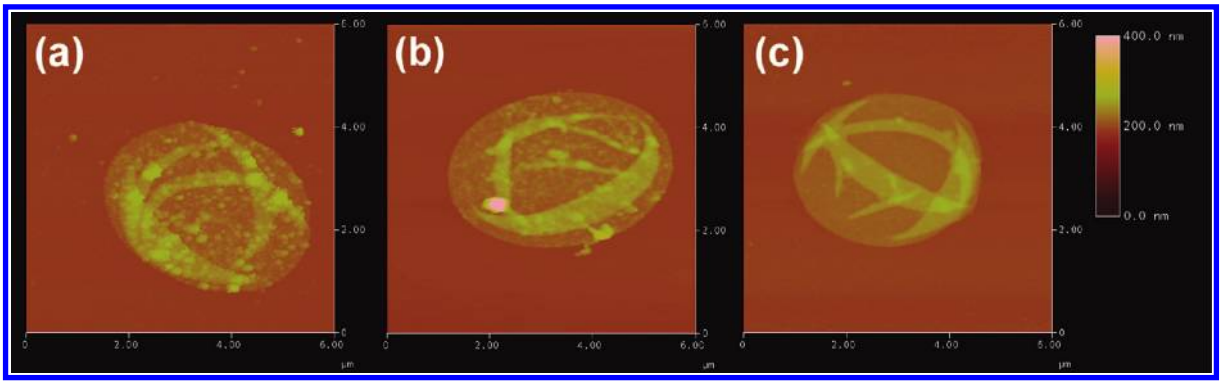

Figure 7. AFM images of PNIPAm microcapsules fabricated at various temperatures and with different compositions: (a) (PNIPAm-Ace_{22}/PNIPAm-Az_{10})$_2$ at 25 °C; (b) (PNIPAm-Ace_{22}/PNIPAm-Az_{22})$_2$ at 20 °C; (c) (PNIPAm-Ace_{22}/PNIPAm-Az_{10})$_1$ at 30 °C.

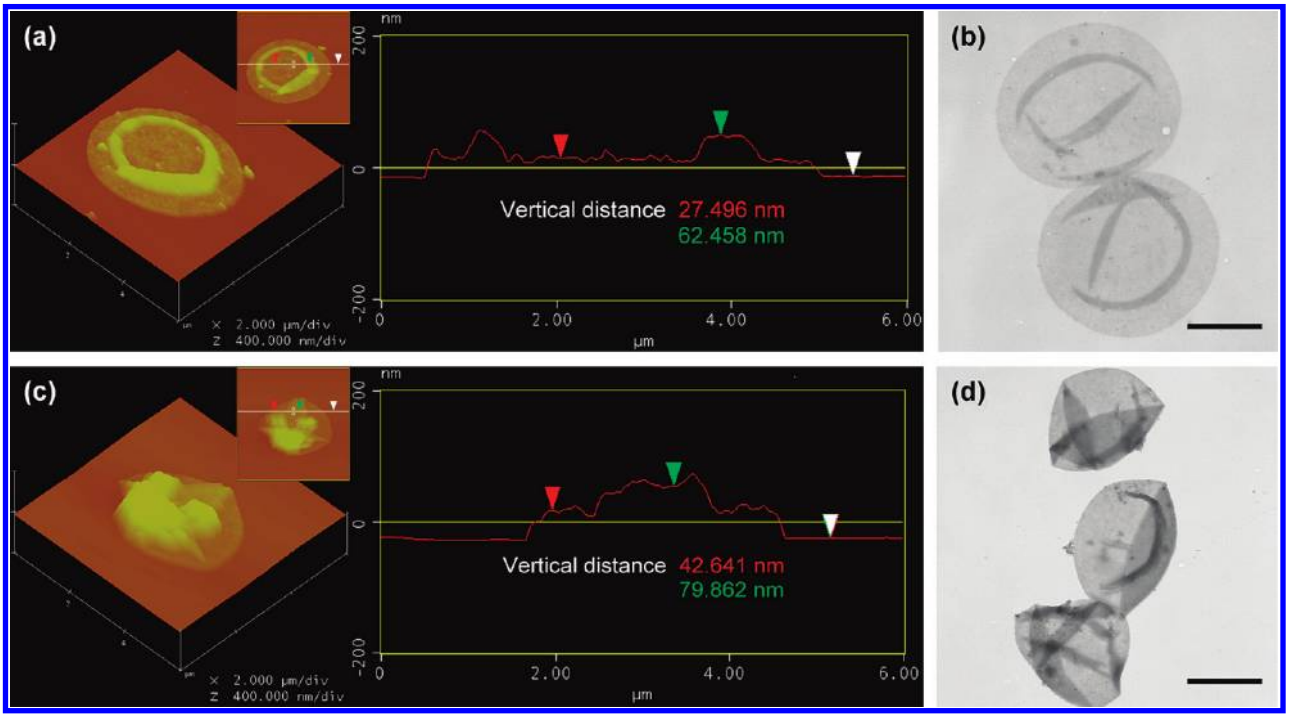

Figure 8. (a, c) AFM and (b, d) TEM images of the two-bilayer (PNIPAm-Ace_{22}/PNIPAm-Az_{10})$_2$ microcapsules assembled closely to LCST at 30 °C. Samples prepared at 25 °C (a, b) and at 50 °C (c, d); the scale bar: 2 μm.

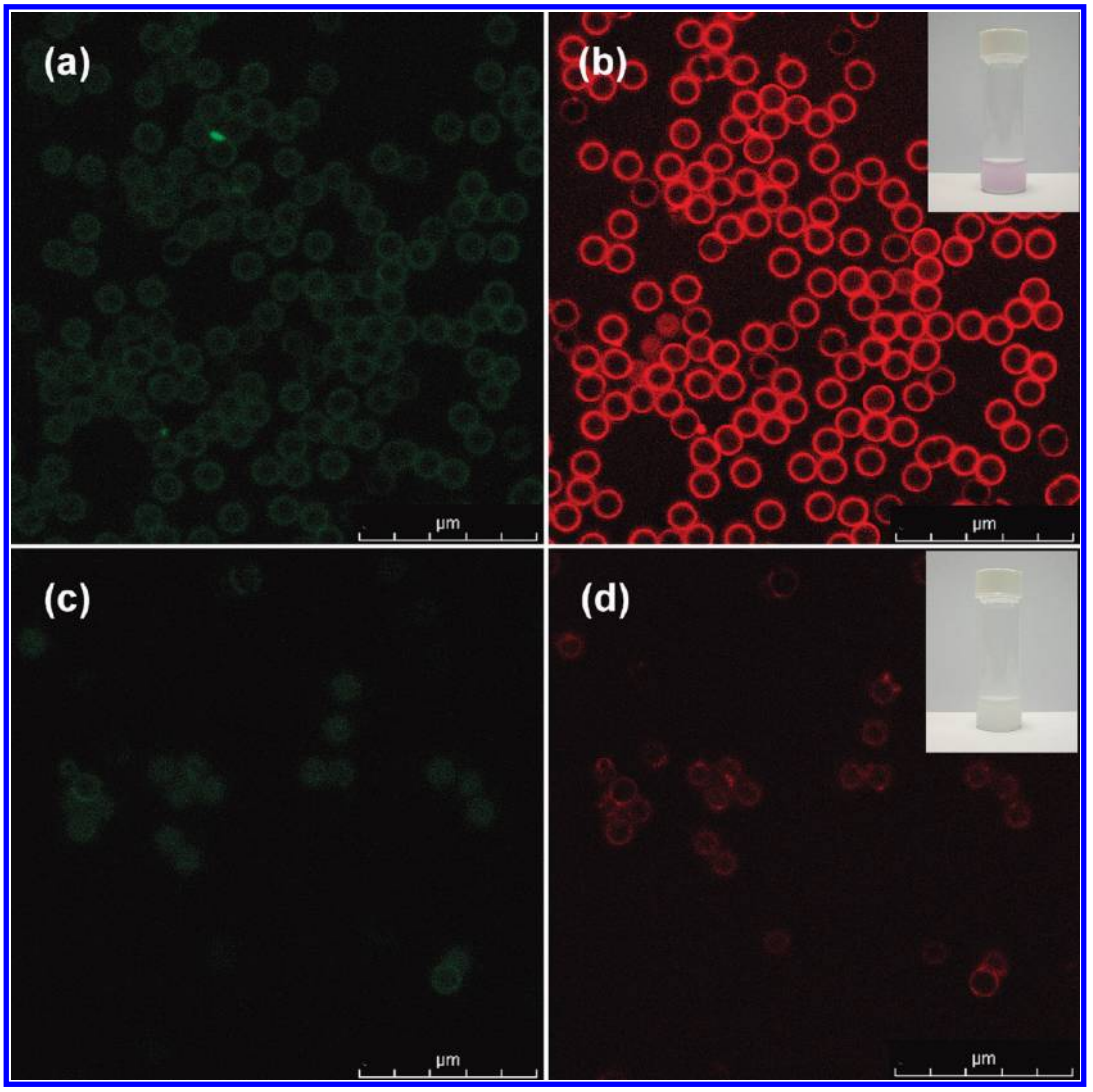

Figure 9. CLSM images of (a, b) three-layer (PNIPAm-Ace$_{22}$/PNIPAm-Az$_{22}$)PNIPAm-Ace$_{22}$ and (c, d) four-layer (PNIPAm-Ace$_{22}$/PNIPAm-Az$_{22}$)$_2$-coated silica particles functionalized with azido-modified lissamine rhodamine dye. The insets of panels b and d show photographs of vials containing lissamine rhodamine surface-modified PNIPAm-coated silica particles suspension. Excitation wavelength (a, c) 403 nm and (b, d) 561 nm; the scale bar: 20 μm.

PNIPAm films is performed is another important factor affecting the morphologies of the resulting thin films. Quinn et al. demonstrated that the adsorption temperature of PNIPAm on planar templates was affected significantly by both the mass proportion of PNIPAm in the film and the morphology of the film's surface;[48] when the adsorption was conducted at temperatures close to the LCST, the amount of PNIPAm in the film increased significantly and the total film mass increased. Using the same concept in this study, we examined the effect of the temperature on the covalent assembly on the colloidal template. Figure 7 displays AFM images of the surface roughnesses of three microcapsule samples assembled with different compositions and at different temperatures. The microcapsule with two PNIPAm-Ace$_{22}$/PNIPAm-Az$_{10}$ bilayers assembled at 25 °C Figure 7a) features numerous polymer grains on the surface; i.e., it possessed a coarse morphology. Increasing the degree of cross-linking resulted in a microcapsule having a smoother surface morphology, as demonstrated by the AFM image of a two-bilayer thin film prepared from PNIPAm-Ace$_{22}$/PNIPAm-Az$_{22}$ (Figure 7b). The formation of polymer grains on the surface can be attributed to the lack of a sufficient number of the remaining free azide functionalities from PNIPAm-Az$_{10}$ as mentioned above. Surprisingly, when we increased the reaction temperature to 30 °C—close to the LCST of the PNIPAm-Ace$_{22}$/PNIPAm-Az$_{10}$ copolymers—the resulting microcapsule featured only one bilayer, but it displayed a continuous and intact shell structure Figure 7c; thickness: ca. 10 nm). This surface was also smoother than that prepared at lower temperature (cf. Figure 7a,c). These results reveal that when we performed the assembly at temperatures close to the LCST, the resulting microcapsules exhibited extremely smooth surfaces and thicker multilayer thin films because of the tighter packing of the PNIPAm derivative as a result of a more compact chain conformation in aqueous solution.

To further investigate the thermoresponsive deswelling behavior of microcapsules fabricated with more tightly packed multilayers, we recorded AFM and TEM images (Figure 8) of the microcapsules possessing two bilayers of PNIPAm-Ace$_{22}$/PNIPAm-Az$_{10}$ that had been assembled at 30 °C. When comparing the AFM images and the height measurements of the microcapsules in their air-dried and thermally dried states Figure 8a,c), we observe a clear increase in the thickness of the thin film—with a size variation confirming that the microcapsule deswelled and shrank—when the microcapsules were dried at 50 °C in the oven. In addition, the TEM images in Figure 8b,d provide

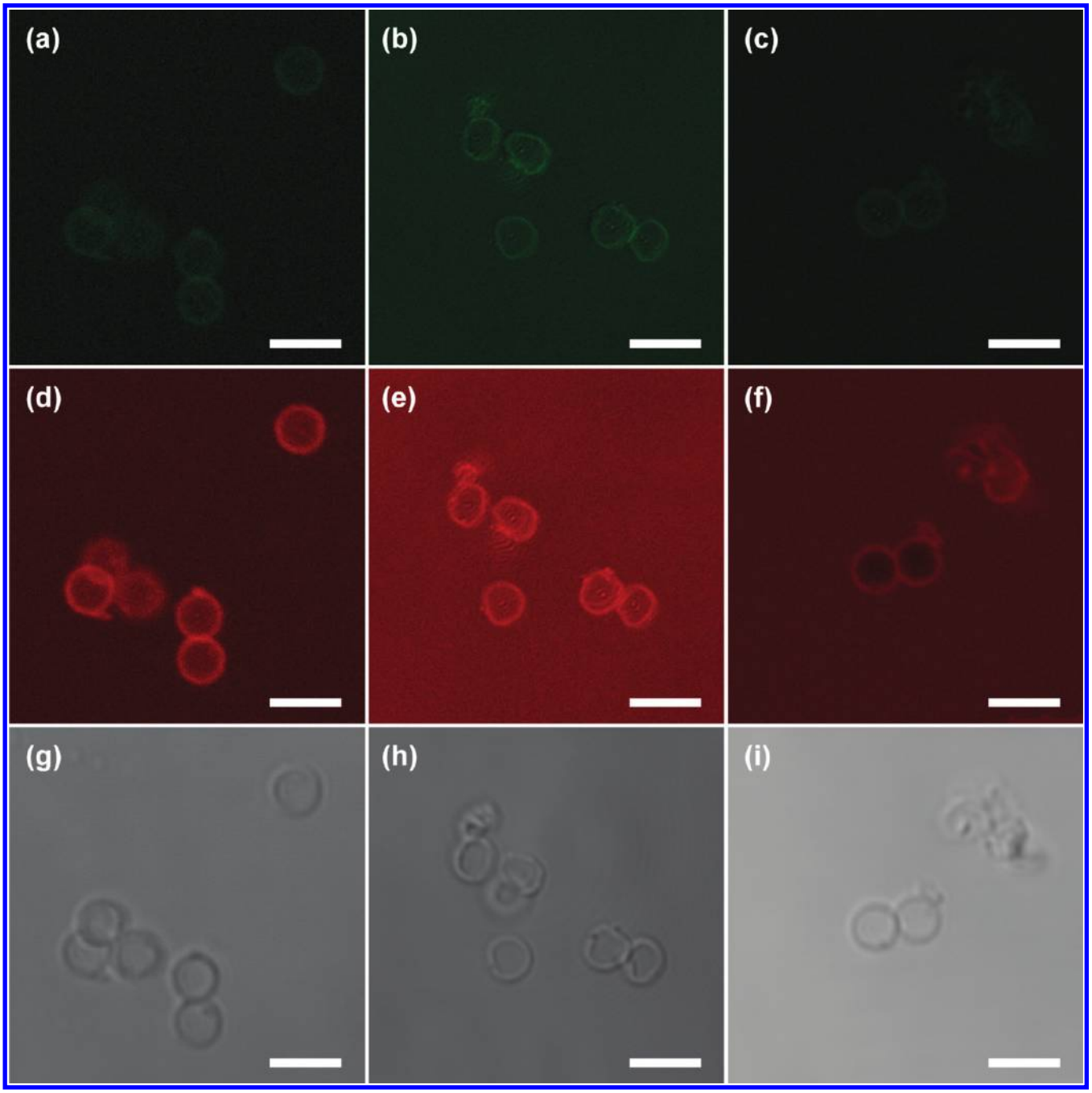

Figure 10. CLSM and DIC images of the two-bilayer (PNIPAm-Ace_{22}/PNIPAm-Az_{10})$_2$ PNIPAm microcapsules assembled at 30 °C after mixing with probe molecule solutions of (a, d, g) rhodamine 6G and TRITC-dextran (b, e, h) $M_w \sim 4.4$ kDa, (c, f, i) $M_w \sim 6.5-7.6$ kDa. Excitation wavelength (a, b, c) 403 nm and (d, e, f) 561 nm; the scale bar: 5 μm.

additional evidence suggesting that the dimensions of the microcapsule decreased considerably upon increasing the temperature above its LCST. To examine the important thermoreversible characteristics, we conducted the heating/cooling processes of the microcapsules suspension solution between 50 and 25 °C repeatedly. As shown in Figure S1 (see Supporting Information), the dimension variation of these microcapsules remained distinguishable between the swelling and deswelling states even after five heating/cooling cycles. This result reveals that the microcapsules show good thermoreversible characteristics in the swelling/deswelling behavior of the ultrathin PNIPAm microcapsules.

Postfunctionalization of PNIPAm Clicked Thin Films through Click Reactions with a Fluorogenic Small Molecule and Preliminary Permeability Study. Because our direct covalent LbL assembly process is based on alternating reactions between remaining free clickable groups on the surface and their complementary copolymers, the presence of unreacted free acetylene or azide moieties can be used for further conjugation with functional materials. To examine the potential for postfunctionalization, we reacted the three-layer (PNIPAm-Ace_{22}/PNIPAm-Az_{22})PNIPAm-Ace_{22}-coated silica particles with a small fluorogenic molecule, namely an azido-modified lissamine rhodamine dye. We then used CLSM to analyze the postfunctionalized silica particles by simultaneously exciting the fluorescent dansyl-labeled PNIPAm thin films and the rhodamine molecules on the surface at excitation wavelengths of 403 and 561 nm, respectively. Figure 9a,b reveals that both green and red fluorescence emissions were visible from the thin films on the

periphery of the silica particles. In order to demonstrate that the unreacted free clickable group is affected at the outer surface, the four-layer coated silica particles (with azide functional group on the surface) were also reacted with the azide-modified rhodamine dye (Figure 9c,d). CLSM analyses show that weak rhodamine fluorescence emission was visible when compared to the three-layer surface-modified silica particles. This result indicates that the clickable group is exclusively affected at the outer surface of the click multilayer, and only few reactive groups remain inside the multilayer thin film. These experiments further demonstrate that the clickable functionalities on the multilayer thin films surface are accessible after each click assembly. Consequently, the microcapsules fabricated through direct covalent LbL assembly allow the surface for postfunctionalization to conjugate a variety of small molecules or larger biomacromolecules.[49] Finally, preliminary study on the permeability of two-bilayer (PNIPAm-Ace_{22}/PNIPAm-Az_{10})$_2$ microcapsule assembled at 30 °C was presented and shown in Figure 10. For microcapsules incubated with probe molecules, rhodamine 6G, or 4.4 kDa TRITC-labeled dextran, it was found that theses microcapsules had the same fluorescence intensity inside as the bulk solution (Figure 10a−f), implying that these low-molecular-weight probe molecules can penetrate into these microcapsules. When the microcapsules incubated with high-molecular-weight TRITC-labeled dextran (65 kDa), however, the dark appearance of capsules interior contrasted with the bright fluorescent outside (Figure 10g−i). These results reveal that the microcapsules with tighter packing wall are selectively permeable to molecules and show potential applications for the encapsulation of variety of materials.

Conclusion

Using click chemistry, we have developed a novel approach to fabricate thermoresponsive PNIPAm microcapsules based on direct covalent bonding LbL assembly. This method not only provides a unique approach toward microcapsule construction with direct covalent bonding under mild reaction conditions but also opens a platform to better understand the effects of the degree of cross-linking on the thin film thickness and morphology. The fabrication of these microcapsules can be tailored by adjusting the aqueous reaction temperature close to the LCST (30 °C), resulting in multilayer film materials exhibiting extremely low surface roughness and high thickness as a result of tighter packing of PNIPAm, a special characteristic of the LbL assembly of PNIPAm on the colloidal template. These microcapsules also undergo a thermoreversible swelling/deswelling transition upon changing the temperature of the medium. The surfaces of these multilayer thin films are easily modified using, for example, an azido-modified lissamine rhodamine dye, thereby allowing post-functionalization with a variety of small molecules or larger biomacromolecules. Finally, permeability study reveals that the microcapsules with tighter packing wall are selectively permeable to molecules depending on molecular weight and show potential applications for the encapsulation of a variety of materials.

Acknowledgment. This study was supported financially by the Ministry of Education's "Aim for the Top University Plan" program and the National Science Council, Taiwan (Contract NSC-97-2220-E-009-003). We are grateful to the staff of TC5 Bio-Image Tools, Technology Commons, College of Life Science, NTU, for help with the CLSM instrument (Leica TCS SP5).

Supporting Information Available: TEM images of the two-bilayer (PNIPAm-Ace_{22}/PNIPAm-Az_{10})$_2$ microcapsules after five heating/cooling cycles between 50 and 25 °C. This material is available free of charge via the Internet at http://pubs.acs.org.

References and Notes

(1) (a) Wang, Y.; Bansal, V.; Zelikin, A. N.; Caruso, F. *Nano Lett.* **2008**, *8*, 1741–1745. (b) Tamber, H.; Johansen, P.; Merkle, H. P.; Gander, B. *Adv. Drug Delivery Rev.* **2005**, *57*, 357–376. (c) Trehan, A.; Sinha, V. R. *J. Controlled Release* **2003**, *90*, 261–280.
(2) (a) Zelikin, A. N.; Becker, A. L.; Johnston, A. P. R.; Wark, K. L.; Turatti, F.; Caruso, F. *ACS Nano* **2007**, *1*, 63–69. (b) Zelikin, A. N.; Li, Q.; Caruso, F. *Angew. Chem., Int. Ed.* **2006**, *45*, 7743–7745.
(3) (a) Molvinger, K.; Quignard, F.; Brunel, D. B.; Angelatos, A. S.; Radt, B.; Caruso, F. *J. Phys. Chem. B* **2005**, *109*, 3071–3076.
(4) (a) Nayak, S.; Gan, D.; Serpe, M. J.; Lyon, L. A. *Small* **2005**, *1*, 416–421. (b) Sun, Q.; Deng, Y. *J. Am. Chem. Soc.* **2005**, *127*, 8274–8275. (c) Qian, J.; Wu, F. *Chem. Mater.* **2007**, *19*, 5839–5841. (d) Zha, L.; Zhang, Y.; Yang, W.; Fu, S. *Adv. Mater.* **2002**, *14*, 1090–1092. (e) Zhang, Y.; Jiang, M.; Zhao, J.; Ren, X.; Chen, D.; Zhang, G. *Adv. Funct. Mater.* **2005**, *15*, 695–699. (f) Glinel, K.; Sukhorukov, G. B.; Mohwald, H.; Khrenov, V.; Tauer, K. *Macromol. Chem. Phys.* **2003**, *204*, 1784–1790.
(5) (a) Sukhishvili, S. A.; Granick, S. *J. Am. Chem. Soc.* **2000**, *122*, 9550–9551. (b) Kozlovskaya, V.; Kharlampieva, E.; Mansfield, M. L.; Sukhishvili, S. A. *Chem. Mater.* **2006**, *18*, 328–336. (c) Such, G. K.; Tjipto, E.; Postma, A.; Johnston, A. P. R.; Caruso, F. *Nano Lett.* **2007**, *7*, 1706–1710. (d) Feng, Z.; Wang, Z.; Gao, C.; Shen, J. *Chem. Mater.* **2007**, *19*, 4648–4657.
(6) (a) Molvinger, K.; Quignard, F.; Brunel, D.; Boissiere, M.; Devoissèlle, J.-M. *Chem. Mater.* **2004**, *16*, 3367–3372. (b) Zhang, J.; Xu, S.; Kumacheva, E. *J. Am. Chem. Soc.* **2004**, *126*, 7908–7914.
(7) (a) Peyratout, C. S.; Dahne, L. *Angew. Chem., Int. Ed.* **2004**, *43*, 3762–3783. (b) Johnston, A. P. R.; Cortez, C.; Angelatos, A. S.; Caruso, F. *Curr. Opin. Colloid Interface Sci.* **2006**, *11*, 203–209. (c) Quinn, J. F.; Johnston, A. P. R.; Such, G. K.; Zelikin, A. N.; Caruso, F. *Chem. Soc. Rev.* **2007**, *36*, 707–718. (d) Sukhorukov, G.; Fery, A.; Mohwald, H. *Prog. Polym. Sci.* **2005**, *30*, 885–897.
(8) (a) Caruso, F.; Caruso, R. A.; Mohwald, H. *Science* **1998**, *282*, 1111–1114. (b) Donath, E.; Sukhorukov, G. B.; Caruso, F.; Davis, S. A.; Mohwald, H. *Angew. Chem., Int. Ed.* **1998**, *37*, 2202–2205.
(9) Decher, G.; Schlenoff, J. *Multilayer Thin Films*; Wiley-VCH: Weinheim, Germany, 2003.
(10) (a) Zhang, Y. J.; Guan, Y.; Yang, S. G.; Xu, J.; Han, C. C. *Adv. Mater.* **2003**, *15*, 832–835. (b) Kozlovskaya, V.; Ok, S.; Sousa, A.; Libera, M.; Sukhishvili, S. A. *Macromolecules* **2003**, *36*, 8590–8592. (c) Yang, S. Y.; Lee, D.; Cohen, R. E.; Rubner, M. F. *Langmuir* **2004**, *20*, 5978–5981.
(11) Wang, Z.; Feng, Z.; Gao, C. *Chem. Mater.* **2008**, *20*, 4194–4199.
(12) (a) Johnston, A. P. R.; Read, E. S.; Caruso, F. *Nano Lett.* **2005**, *5*, 953–956. (b) Johnston, A. P. R.; Mitomo, H.; Read, E. S.; Caruso, F. *Langmuir* **2006**, *22*, 3251–3258.
(13) (a) Liu, Y. L.; Bruening, M. L.; Bergbreiter, D. E.; Crooks, R. M. *Angew. Chem., Int. Ed.* **1997**, *36*, 2114–2116. (b) Major, J. S.; Blanchard, G. J. *Langmuir* **2001**, *17*, 1163–1168. (c) Serizawa, T.; Matsukuma, D.; Nanemeki, K.; Uemura, M.; Kurusu, F.; Akashi, M. *Macromolecules* **2004**, *37*, 6531–6536. (d) Liang, Z.; Wang, Q. *Langmuir* **2004**, *20*, 9600–9606. (e) Tian, Y.; He, Q.; Tao, C.; Li, J. *Langmuir* **2006**, *22*, 360–362. (f) Buck, M. E.; Zhang, J.; Lynn, D. M. *Adv. Mater.* **2007**, *19*, 3951–3955.
(14) Moya, S.; Dahne, L.; Voigt, A.; Leporatti, S.; Donath, E.; Mohwald, H. *Colloids Surf., A* **2001**, *183−185*, 27–40.
(15) (a) Nardin, C.; Hirt, T.; Leukel, J.; Meier, W. *Langmuir* **2000**, *16*, 1035–1041. (b) Pastoriza-Santos, I.; Scholer, B.; Caruso, F. *Adv. Funct. Mater.* **2001**, *11*, 122–128. (c) Zhu, H. G.; McShane, M. J. *Langmuir* **2005**, *21*, 424–430.
(16) (a) Tong, W. J.; Gao, C. Y.; Mohwald, H. *Chem. Mater.* **2005**, *17*, 4610–4616. (b) Zhang, Y. J.; Guan, Y.; Zhou, S. *Biomacromolecules* **2005**, *6*, 2365–2369.
(17) (a) Schuetz, P.; Caruso, F. *Adv. Funct. Mater.* **2003**, *13*, 929–937. (b) Kozlovskaya, V.; Ok, S.; Sousa, A.; Libera, M.; Sukhishvili, S. A. *Macromolecules* **2003**, *36*, 8590–8592. (c) Lee, D.; Rubner, M. F.; Cohen, R. E. *Chem. Mater.* **2005**, *17*, 1099–1105. (d) Yang, S. Y.; Lee, D.; Cohen, R. E. *Langmuir* **2004**, *20*, 5978–6981.
(18) (a) Feng, Z.; Wang, Z.; Gao, C.; Shen, J. *Adv. Mater.* **2007**, *19*, 3687–3691. (b) Tong, W.; Gao, C.; Mohwald, H. *Macromol. Rapid Commun.* **2006**, *27*, 2078–2083. (c) Duan, L.; He, Q.; Yan, X. H.;

Cui, Y.; Wang, K. W.; Li, J. B. *Biochem. Biophys. Res. Commun.* **2007**, *354*, 357–362.
(19) (a) Zelikin, A. N.; Quinn, J. F.; Caruso, F. *Biomacromolecules* **2006**, *7*, 27–30. (b) Zelikin, A. N.; Li, Q.; Caruso, F. *Angew. Chem., Int. Ed.* **2006**, *45*, 7743–7745. (c) Zelikin, A. N.; Li, Q.; Caruso, F. *Chem. Mater.* **2008**, *20*, 2655–2661.
(20) (a) Such, G. K.; Quinn, J. F.; Quinn, A.; Tjipto, E.; Caruso, F. *J. Am. Chem. Soc.* **2006**, *128*, 9318–9319. (b) Such, G. K.; Tjipto, E.; Postma, A.; Johnston, A. P. R.; Caruso, F. *Nano Lett.* **2007**, *7*, 1706–1710. (c) Ochs, C. J.; Such, G. K.; Stadler, B.; Caruso, F. *Biomacromolecules* **2008**, *9*, 3389–3396.
(21) (a) Kolb, H. C.; Finn, M. G.; Sharpless, K. B. *Angew. Chem., Int. Ed.* **2001**, *40*, 2004–2021. (b) Kolb, H. C.; Sharpless, K. B. *Drug Discovery Today* **2003**, *8*, 1128–1137. (c) Lewis, W. G.; Green, L. G.; Grynszpan, F.; Radic, Z.; Carlier, P. R.; Taylor, P.; Finn, M. G.; Sharpless, K. B. *Angew. Chem., Int. Ed.* **2002**, *41*, 1053–1057. (d) Hawker, C. J.; Wooley, K. L. *Science* **2005**, *309*, 1200–1205.
(22) (a) Huisgen, R. *Angew. Chem., Int. Ed.* **1968**, *7*, 321–328. (b) Bock, V. D.; Hiemstra, H.; van Maarseveen, J. H. *Eur. J. Org. Chem.* **2006**, 51–68.
(23) Schild, H. G. *Prog. Polym. Sci.* **1992**, *17*, 163–249.
(24) (a) Pelton, R. H.; Chibante, P. *Colloids Surf.* **1986**, *20*, 247–256. (b) Zhang, J.; Pelton, R.; Deng, Y. *Langmuir* **1995**, *11*, 2301–2302.
(25) Zha, L. S.; Zhang, Y.; Yang, W. L.; Fu, S. K. *Adv. Mater.* **2002**, *14*, 1090–1092.
(26) (a) Nayak, S.; Gan, D. J.; Serpe, M. J.; Lyon, L. A. *Small* **2005**, *1*, 416–421. (b) Zhang, Y. W.; Jiang, M.; Zhao, J. X.; Ren, X. W.; Cheng, D. Y.; Zhang, G. Z. *Adv. Funct. Mater.* **2005**, *15*, 695–699. (c) Qian, J.; Wu, F. *Chem. Mater.* **2007**, *19*, 5839–5841.
(27) Glinel, K.; Sukhorukov, G. B.; Mohwald, H.; Khrenov, V.; Tauer, K. *Macromol. Chem. Phys.* **2003**, *204*, 1784–1790.
(28) (a) Sun, Q. H.; Deng, Y. L. *J. Am. Chem. Soc.* **2005**, *127*, 8274–8275. (b) Cheng, C.-J.; Chu, L.-Y.; Ren, P.-W.; Zhang, J.; Hu, L. *J. Colloid Interface Sci.* **2007**, *313*, 383–388. (c) Lawrence, D. B.; Cai, T.; Hu, Z.; Marquez, M.; Dinsmore, A. D. *Langmuir* **2007**, *23*, 395–398.
(29) (a) Lutz, J. F. *Angew. Chem., Int. Ed.* **2007**, *46*, 1018–1025. (b) Binder, W. H.; Sachsenhofer, R. *Macromol. Rapid Commun.* **2007**, *28*, 15–54. (c) Fournier, D.; Hoogenboom, R.; Schubert, U. S. *Chem. Soc. Rev.* **2007**, *36*, 1369–1380. (d) Golas, P. L.; Matyjaszewski, K. *QSAR Comb. Sci.* **2007**, *11*−*12*, 1116–1134.
(30) (a) Binder, W. H.; Kluger, C. *Macromolecules* **2004**, *37*, 9321–9330. (b) Binder, W. H.; Kluger, C.; Josipovic, M.; Straif, C. J.; Friedbacher, G. *Macromolecules* **2006**, *39*, 8092–8101.
(31) Malkoch, M.; Thibault, R. J.; Drockenmuller, E.; Messerschmidt, M.; Voit, B.; Russell, T. P.; Hawker, C. J. *J. Am. Chem. Soc.* **2005**, *127*, 14942–14949.
(32) Luxenhofer, R.; Jordan, R. *Macromolecules* **2006**, *39*, 3509–3516.
(33) (a) Sumerlin, B. S.; Tsarevsky, N. V.; Louche, G.; Lee, R. Y.; Matyjaszewski, K. *Macromolecules* **2005**, *38*, 7540–7545. (b) Ladmiral, V.; Mantovani, G.; Clarkson, G. J.; Cauet, S.; Irwin, J. L.; Haddleton, D. M. *J. Am. Chem. Soc.* **2006**, *128*, 4823–4830. (c) Zhang, J.; Zhou, Y.; Zhu, Z.; Ge, Z.; Liu, S. *Macromolecules* **2008**, *41*, 1444–1454.
(34) (a) Riva, P.; Schmeits, S.; Stoffelbach, F.; Jérôme, C.; Jérôme, R.; Lecomte, P. *Chem. Commun.* **2005**, 5334–5336. (b) Lecomte, P.; Riva, P.; Schmeits, S.; Rieger, J.; Butsele, K. V.; Jérôme, C.; Jérôme, R. *Macromol. Symp.* **2006**, *240*, 157–165.
(35) Ciampolini, M.; Nardi, N. *Inorg. Chem.* **1966**, *5*, 41–44.
(36) Carboni, B.; Benanlil, A.; Vaultier, M. *J. Org. Chem.* **1993**, *58*, 3736–3741.
(37) Rozkiewicz, D.; Janczewski, D.; Verboom, W.; Ravoo, B. J.; Reinhoudt, D. N. *Angew. Chem., Int. Ed.* **2006**, *45*, 5292–5296.
(38) Gujadhur, R.; Venkataraman, D.; Kintigh, J. T. *Tetrahedron Lett.* **2001**, *42*, 4791–4793.
(39) Ranjan, R.; Brittain, W. J. *Macromolecules* **2007**, *40*, 6217–6223.
(40) Bergbreiter, D. E.; Chance, B. S. *Macromolecules* **2007**, *40*, 5337–5343.
(41) Huang, C.-J.; Chang, F.-C. *Macromolecules* **2008**, *41*, 7041–7052.
(42) Jiang, X.; Zhang, J.; Zhou, Y.; Xu, J.; Liu, S. *J. Polym. Sci., Part A: Polym. Chem.* **2008**, *46*, 860–871.
(43) Opsteen, J. A.; van Hest, J. C. M. *Chem. Commun.* **2005**, 57–59.
(44) Feil, H.; Bae, Y. H.; Feijen, J.; Kim, S. W. *Macromolecules* **1993**, *26*, 2496–2500.
(45) (a) Chen, G.; Hoffman, A. S. *Macromol. Chem. Phys.* **1995**, *196*, 1251–1259. (b) Kuckling, D.; Adler, H.-J.; Arndt, K.-F.; Ling, L.; Habicher, W. D. *Macromol. Symp.* **1999**, *145*, 65–74. (c) Kunugi, S.; Yamazaki, Y.; Takano, K.; Tanaka, N. *Langmuir* **1999**, *15*, 4056–4061. (d) Deng, Y.; Pelton, R. *Macromolecules* **1995**, *28*, 4617–4621.
(46) Kuckling, D.; Adler, H.-J. P.; Arndt, K.-F.; Ling, L.; Habicher, W. D. *Macromol. Chem. Phys.* **2000**, *201*, 273–280.
(47) (a) Hoare, T.; Pelton, R. *Macromolecules* **2004**, *37*, 2544–2550. (b) Jones, C. D.; Lyon, L. A. *Macromolecules* **2003**, *36*, 1988–1993.
(48) (a) Quinn, J. F.; Caruso, F. *Langmuir* **2004**, *20*, 20–22. (b) Kharlampieva, E.; Kozlovskaya, V.; Ankner, J. F.; Sukhishvili, S. A. *Langmuir* **2008**, *24*, 11346–11349.
(49) Nystrom, A. M.; Wooley, K. L. *Tetrahedron* **2008**, *64*, 8543–8552.